

Weighing the Axion with Muon Haloscopy

N. Bray-Ali*

*Department of Physical Sciences
Mount Saint Mary's University
12001 Chalon Rd.*

Los Angeles, CA 90049

(Dated: September 13, 2022)

Axions in the local dark matter halo of the galaxy collide with virtual photons dressing the electromagnetic vertex of the muon. The collisions shift the muon magnetic moment in a way that scales with the volume of the muon beam and transforms like the axion under the charge conjugation, parity, and time-reversal symmetries of electromagnetism. Analysis of measurements of the muon magnetic moment suggests that axions saturate the local halo energy density and that the axion shift resolves the tension between the measurements and the Standard Model of particle physics provided axions have the mass suggested by a symmetry argument. Table-top experiments for measuring the mass of the axion directly are proposed.

I. INTRODUCTION

The spin of the muon precesses in a magnetic field B at frequency $\omega_a = a_\mu(e/m_\mu)B$, where, $a_\mu \approx \alpha/(2\pi) \approx 1.16 \times 10^{-3}$, and $e/m_\mu = 2\pi \times 135$ MHz/T is the charge to mass ratio of the muon [1–4]. Compared with the electron, the muon is $(m_\mu/m_e)^2 \approx 43,000$ times more sensitive to the hadronic leading order contribution a_μ^{HLO} to spin precession [5, 6]. In this Letter, we show that axions in the local dark matter halo of the galaxy shift a_μ from the standard model values in a way that scales with the volume of the “haloscope” and that transforms like the axion under the charge conjugation C , parity P , and time-reversal T symmetries of electromagnetism[7].

II. AXION MASS

We start by expressing the axion A_M in terms of quarks and leptons M_H^P with helicity $H = L, R$ and charge-parity check $P = +, -$ [8]:

$$A_M = M_L^- \bar{M}_R^- - M_R^- \bar{M}_L^- - M_L^+ \bar{M}_R^+ + M_R^+ \bar{M}_L^+ \quad (1)$$

Here, M runs over the twelve known “flavors” of quarks and leptons while the charge-parity check P is $+$ for quarks and leptons that do not feel the weak nuclear force and $-$ for those that do. In the standard model, we find M_L^- and M_R^+ , but neither M_L^+ nor M_R^- , where, L is for left-handed and R is for right-handed helicity [9].

Next, we suppose that axions A_M of each kind and photons γ_H of each helicity formed in equal numbers in the early universe prior to baryogenesis. This fixes the ratio $n_A/n_\gamma = |M|/|H| = 6$ of axions to photons and gives the axion mass m_A ($\hbar = c = 1$) [10]:

$$m_A = 2.70 \text{ kT}_\gamma \left(\frac{n_A}{n_\gamma} \right)^{-1} \frac{\Omega_A h^2}{\Omega_\gamma h^2} = (0.508 \pm 0.004) \text{ eV}, \quad (2)$$

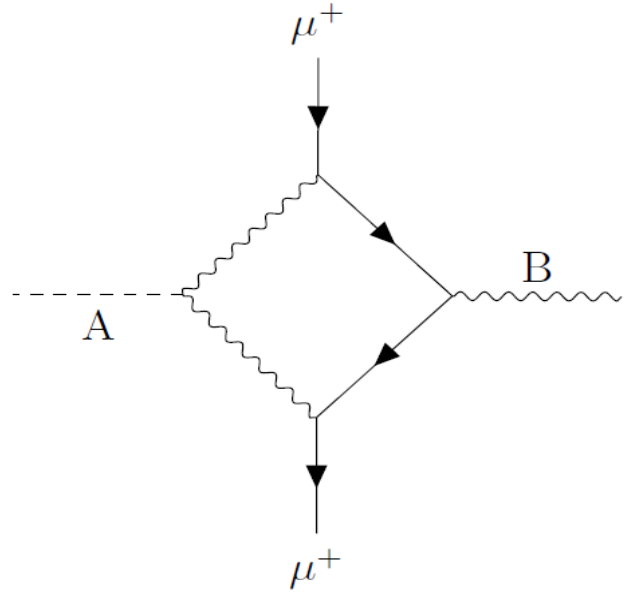


FIG. 1. Halo axion A collides with virtual photon or vector meson dressing vertex of positive muon μ^+ and magnetic field B .

where, $T_\gamma = (2.7255 \pm 0.0006)$ K is the present photon temperature[11], $\Omega_\gamma h^2 = 2.473 \times 10^{-5}$ is the photon energy density parameter and $\Omega_A h^2 = 0.11882 \pm 0.0086$ is that of the axions assuming they saturate the dark matter [12].

III. MUON HALOSCOPY

Figure 1 shows how axions in the local halo shift muon spin precession [2–4]. Acting as a background field $\tilde{\phi}_A(q_A)$ with on-shell four-momentum $q_A^2 = m_A^2 \ll m_\mu^2$, the axion A couples to the virtual photon dressing the vertex of the positive muon μ^+ and the magnetic field

* nbrayali@msmu.edu

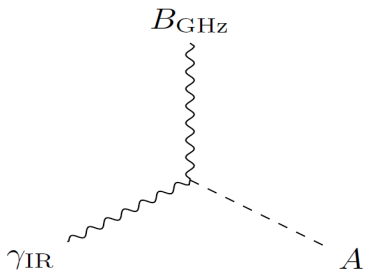


FIG. 2. Halo axion A converts infrared photon γ_{IR} into gigahertz frequency magnetic field B_{GHz}

B. The shift of the spin precession frequency Δa_μ grows with the axion-photon coupling $g_{A\gamma\gamma}$ [13]:

$$\frac{\Delta a_\mu}{a_\mu} = m_A^2 g_{A\gamma\gamma} \tilde{\phi}_A(q_A) = \pm m_A g_{A\gamma\gamma} \sqrt{\rho_A N_\mu V_\mu T_\mu} \quad (3)$$

where, the axion field strength $|\tilde{\phi}_A(q_A)|^2 \approx \phi_A^2 N_\mu V_\mu T_\mu$ is fixed by the axion energy density $\rho_A = \phi_A^2 m_A^2$, the volume V_μ of the muon beam, the lifetime T_μ of the muon in the axion rest-frame, and the average number of muons N_μ during spin precession. The sign of the shift Δa_μ in Eq. (3) switches along with the axion field $\tilde{\phi}_A(q_A)$ under the symmetries P , T , CP , and CT [14]. The size of the shift scales with the effective four-volume NVT of the muon beam. This is our main result.

The shift in the muon spin precession frequency Δa_μ due to axions in the local dark matter halo of the galaxy has roughly the right size to resolve the tension $a_\mu(\text{Exp}) - a_\mu(\text{SM}) = (251 \pm 59) \times 10^{-11}$ between experiments (Exp) [2, 3] and standard model calculations (SM) [5, 6]. Assuming axions saturate the local halo, their energy density $\rho_A = (0.30 \pm 0.03) \text{ GeV/cm}^3$ follows from galactic orbital dynamics and other astrophysical constraints [15]. Similarly, the axion-photon coupling strength $|g_{A\gamma\gamma}| = (0.75 \pm 0.08) \times 10^{-10} \text{ GeV}^{-1}$ is given by observations of giant stars in globular clusters [16] assuming they had the same helium abundance in their cores when they formed as the sun did when it formed [17]. Combining these astrophysical inputs with the axion mass $m_A = (0.508 \pm 0.004) \text{ eV}$ from cosmological considerations and symmetry arguments (See Eq. 2), we find the size of the shift $|\Delta a_\mu| = (187 \pm 23) \times 10^{-11}$ of the muon spin precession frequency due to axions in the local dark matter halo of the galaxy roughly resolves the tension between experiment and the standard model [18].

Figure 1 also shows how axions from the local dark matter halo of the galaxy shift measurements of the leading order hadronic contribution a_μ^{HLO} to muon spin precession [4, 5]. The axions collide with the ρ vector meson that dominates the hadronic production from electron-positron annihilation whose cross-section enters the standard model calculation of a_μ^{HLO} . The collisions convert the short-lived ρ meson, which produces mainly charged pion $\pi^+\pi^-$ pairs, into the longer lived and slightly heavier ω meson, which prefers to produce a neutral pion π^0 in

addition to the charged pion pair. The conversions reduce the $\pi^+\pi^-$ hadronic production cross-section at the ρ resonance and increase the systematic uncertainty of the measurement by producing excess $\pi^+\pi^-\pi^0$ events.

The coupling $g_{A\rho\omega}$ between the axion and the vector mesons shown in Fig. 1 leads to a drop $\Delta a_\mu^{\text{HLO}}$ in the calculated value of the leading order hadronic contribution:

$$\begin{aligned} \frac{\Delta a_\mu^{\text{HLO}}}{a_\mu} &= -m_A^2 |g_{A\rho\omega} \tilde{\phi}_A(q_A)| \\ &= -\frac{2\pi}{3} |\Delta a_\mu| \sqrt{\frac{m_\rho m_\omega N_e V_e T_e}{\Gamma_\rho^{ee} \Gamma_\omega^{ee} N_\mu V_\mu T_\mu}}, \end{aligned} \quad (4)$$

where, the mass of vector meson $V = \rho, \omega$ is m_V , the partial width Γ_V^{ee} gives the rate that V produces an electron-positron pair, N_e is the number of electrons and positrons in each colliding bunch, V_e is the luminous volume they create, and T_e is the time it takes the bunches to cross during the collision [21]. Provided the shift Δa_μ in Eq. (3) is positive, the drop $-|\Delta a_\mu^{\text{HLO}}|$ in the hadronic contribution given by Eq. (4) combines to give a gap between experiment and the standard model $\Delta a_\mu + |\Delta a_\mu^{\text{HLO}}| = 1.67 \times \Delta a_\mu = (312 \pm 38) \times 10^{-11}$ that is quite close to the observed tension [24].

IV. INFRARED HALOSCOPY

Figure 2 shows how the axion converts infrared photons into radio-frequency magnetic fields. From Eq. (2) we find the wavelength $\lambda_A = 2\pi/m_A = (2441 \pm 19) \text{ nm}$ corresponding to the mass of the axion falls in the mid-infrared. Detuning the infrared light from λ_A by the ground-state hyperfine transition frequency of an alkali atom, such as cesium-133, we can create radio-frequency magnetic field B_{GHz} within a resonant microwave cavity surrounding a gas vapor cell [26]:

$$|B_{\text{GHz}}| = m_A^2 |g_{A\gamma\gamma} E_{\text{IR}} \tilde{\phi}_A(q_A)| = \frac{|\Delta a_\mu|}{a_\mu} |E_{\text{IR}}| \sqrt{\frac{N V T}{N_\mu V_\mu T_\mu}}. \quad (5)$$

Here, E_{IR} is the infrared electric field, N is the number of gas atoms, V is the volume of the microwave cavity, and T is the cavity life-time. By scanning the infrared wavelength and looking for resonant absorption of the radio-frequency magnetic field by the atoms, it is possible to measure λ_A and hence determine the mass of the axion directly in a table-top experiment.

Figure 3 shows how the axion allows infrared light to excite electromagnons in ferroelectric antiferromagnets such as BiFeO_3 . At room temperature the strongest electromagnon resonance in BiFeO_3 lies in the terahertz regime at frequency $\omega_\theta = 2\pi \times 0.54 \text{ THz}$. With increasing temperature, the electromagnon softens along with the spin density wave amplitude [27]. Looking in the infrared, we expect to see the electromagnon resonance as

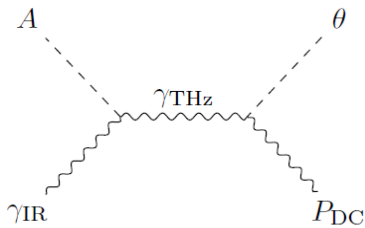


FIG. 3. Halo axion A converts infrared photon γ_{IR} into terahertz photon γ_{THz} resonant with electromagnon θ in ferroelectric antiferromagnet with polarization P_{DC} .

an absorption line in transmission through a thin sample, for example, provided the light is detuned by ω_θ from the axion frequency $\omega_A = m_A = 2\pi \times (122.9 \pm 1.0)$ THz[28]. Measuring the infrared frequency that resonantly excites the electromagnon provides a table-top determination of the mass of the axion.

V. CONCLUSION

We conclude that the tension between measurements of the muon magnetic moment and standard model calculations is due to axions in the local dark matter halo of the galaxy. Comparing the axion shift with the muon tension, we can infer that axions saturate the local halo energy density if we assume the axion has the mass $m_A = (0.508 \pm 0.004)$ eV suggested by symmetry and cosmology. Table-top experiments using readily available materials and devices can directly measure the mass of the axion to confirm this per cent level prediction.

ACKNOWLEDGEMENTS

We thank Daria Mazura, Kevin Njokom, Amolek Virk, David C. Chester, Varsha Subramanian, Peter H. Fisher, Uwe-Jens Wiese, Satoshi Watanabe, Joel E. Moore, Stephan Haas, Ganpathy Murthy, Martin Hoferichter, Graziano Venanzoni, Achim Denig, Christoph Redmer, Ivan Logashenko, Daisuke Nomura, Hoang Nguyen, Klaus Blaum, Stephan Ulmer, Svetljana Fajfer, Howard Baer, James Mott, B. Chris Regan, Y. Guo, M. Kazura, Roy A. Lacey, C. M. Grayson, Gilberto Colangelo, Dominick Stockinger, David W. Hertzog, B. Lee Roberts, Bogdan Malaescu, James M. Cline, Michael Levin, Berndt Mueller, Fiona Kirk, Guido Gagliardi, David d'Enterria, Giulia Zanderighi, Andre H. Hoang, Hannah Binney, Aida X. El-Khadra, Tim Gorringer, Venkatraman Gopalan, Roger D. Blandford, Zoya Vallari, Callum Wilkinson, Jim Freericks, Paul Hamilton, Rahul Roy, Stuart E. Brown, Callum Jones, Kirill Shtengel, Vivek Aji, Per Kraus, Robijn Bruinsma, Anshul Kogar, Chetan Nayak, Zvi Bern, Tsutomu Mibe, Hartmut Wittig, Thomas Blum, Nima Arkani-Hamed, Eric Weinstein, Kei-Fei Liu, Mani Bhaumik, Massimo Passera, Sven Heinemeyer, Juan Maldacena, Phillip Cox, Michael Pomfret, Michael E. Peskin, Sam Posen, Yannis Sermertzidis, Chris Quigg, Gray Rybka, Pavel Nadolsky, Vladimir Shiltsev, Frank Zimmerman, Sergei Nagaitsev, Tom Shutt, Maria Elena Monzani, David McKeen, Josh Berger, Corrine Mills, Sanjay Reddy, George Fuller, Masha Baryakhtar, Charles J. Horowitz, Jiunn-Wei Chen, Jonathen Engel, Arturo R. Samana, Tien-Tien Yu, Peter B. Denton, Arturo R. Samana, Manuel A. Ben-Abad, Ricardo S. Farias, Andrei Derevianko, Dmitry Budker, Harikrishnan Ramani, M. Angeles Perez-Garcia and Peter Athron for insightful correspondence and discussions. This research was supported in part by the National Science Foundation under Grant No. NSF PHY-1748958, by the Department of Energy under grant No. DE-FG02-00ER41132, and by the Mainz Institute of Theoretical Physics within the Cluster of Excellence PRISMA+ (Project ID 39083149).

-
- [1] J. Schwinger, On Quantum-Electrodynamics and the Magnetic Moment of the Electron, *Phys. Rev.* **73**, 416 (1948).
 - [2] B. Abi, T. Albahri, S. Al-Kilani, D. Allspach, L. P. Alonzi *et al.* (Muon $g - 2$ Collaboration), Measurement of the Positive Muon Anomalous Magnetic Moment to 0.46 ppm, *Phys. Rev. Lett.* **126**, 141801 (2021).
 - [3] G.W. Bennett, B. Bousquet, H. N. Brown, G. Bunce, R. M. Carey *et al.* (Muon $g - 2$ Collaboration), Final report of the muon E821 anomalous magnetic moment measurement at BNL, *Phys. Rev. D* **73**, 072003 (2006).
 - [4] F. Jegerlehner, *The Anomalous Magnetic Moment of the Muon*, 2nd ed. (Springer-Verlag, 2017).
 - [5] T. Aoyama, N. Asmussen, M. Benayoun, J. Bijnens, T. Blum *et al.*, The anomalous magnetic moment of the muon in the standard model, *Phys. Rep.* **887**, 1 (2020).
 - [6] Sz. Borsanyi, Z. Fodor, J. N. Guenther, C. Hoelbling, S. D. Katz *et al.*, Leading hadronic contribution to the muon magnetic moment from lattice QCD, *Nature* **593**, 51 (2021).
 - [7] R. D. Peccei, in *CP Violation*, edited by C. Jarlskog (World Scientific, 1989) pp. 516–517.
 - [8] The axions A_M are constructed to transform under C , P , and T as $CA_M = A_M$, $PA_M = -A_M$, and $TA_M = -A_M$. To check that they do so, recall that quarks and leptons M_H^P transforms as $CM_H^P = \overline{M_H^P}$, $PM_H^P = M_H^P$,

- and $TM_H^P = \overline{M_H^P}$.
- [9] For anti-matter, the meaning of the parity check is reversed compared to matter: $P = +$ indicates anti-quarks and anti-leptons which *do* feel the weak force, while $P = -$ means the anti-matter *does not* feel it. Nevertheless, the standard model correlation between helicity $H = L, R$ and parity check $P = +, -$ applies in the same way to anti-matter as it does to matter: $\overline{M_L^-}$ and $\overline{M_R^+}$ occur in the standard model while neither $\overline{M_L^+}$ nor $\overline{M_R^-}$ do. See, for example, M. E. Peskin and D. V. Schroeder, *An Introduction to Quantum Field Theory* (Perseus, 1995) pp. 704–705.
- [10] J. Peebles, *Principles of Physical Cosmology* (Princeton University Press, 1993), pp. 137–138, 158–160.
- [11] D. J. Fixsen, The Temperature of the Cosmic Microwave Background, *Astrophys. J.* **707**, 916 (2009).
- [12] N. Aghanim, Y. Akrami, M. Ashdown, J. Aumont, C. Baccigalupi *et al.* (Planck Collaboration), *Planck* 2018 Results VI. Cosmological Parameters, *A&A* **641**, A6 (2018). We use parameters from the baseline model fit to the most complete combination of available data. The results are given in *Planck* 2018 Results: Cosmological Parameter Tables, pg. 49 (May 14, 2019).
- [13] The axion ϕ_A couples to photons via the term $\mathcal{L}_{A\gamma} = \int d^3x dt g_{A\gamma\gamma} \phi_A \mathbf{E} \cdot \mathbf{B}$ in the action, where, \mathbf{E} is the electric field and \mathbf{B} is the magnetic field. We follow here the conventions of the axion theory review by R. D. Peccei [7] in which the “free” terms in the axion action take the form $\mathcal{L}_A = \int d^3x dt [(1/2)(\partial_t \phi_A)^2 - (1/2)(\nabla \phi_A)^2 - (1/2)m_A^2 \phi_A^2]$.
- [14] Under C , PT and CPT , the shift Δa_μ , like the axion amplitude, does not change sign.
- [15] A.-C. Eilers, D. W. Hogg, H.-W. Rix, and M. K. Ness, The Circular Velocity Curve of the Milky Way from 5 to 25 kpc, *Astrophys. J.*, **871**, 120 (2019).
- [16] A. Ayala, I. Dominguez, M. Giannotti, A. Mirizzi, and O. Straniero, Revisiting the Bound on Axion-Photon Coupling from Globular Clusters, *Phys. Rev. Lett.* **113**, 191302 (2014). They added axions to standard stellar evolution codes and found the “empirical” relation $R = 6.26 Y - 0.41 g_{10}^2 - 0.12$ between core helium mass fraction at formation Y , axion-photon coupling $g_{A\gamma\gamma} = g_{10} \times 10^{-10} \text{ GeV}^{-1}$, and ratio $R = N_{\text{HB}}/N_{\text{RGB}}$ of the number N_{HB} of giant stars in globular clusters burning helium in their core compared to the number N_{RGB} burning hydrogen in a shell around the core. Using observations of 39 globular clusters, they estimated $R = 1.39 \pm 0.03$.
- [17] A. M. Serenelli and S. Basu, Determining the Initial Helium Abundance of the Sun, *Astrophys. J.* **719**, 865 (2010) found $Y_{\odot}^{\text{ini}} = 0.278 \pm 0.006$ for the abundance of helium by mass in the core of the sun at the time of formation.
- [18] For the muon beam at Fermilab E989 (FNAL) [2], the volume is $V = 2\pi^2 R \sigma_x \sigma_y = 3.12 \times 10^4 \text{ cm}^3$, where, $R = 711 \text{ cm}$ is the radius of the central orbit of muons in the ring, $\sigma_x = 1.78 \text{ cm}$ is the radial width of the beam, and $\sigma_y = 1.25 \text{ cm}$ is the vertical width [2, 19, 20]. The average number of muons is $N = \frac{4}{9} N_0 e^{-t_{\text{fill}}/(\gamma\tau_\mu)} \approx \frac{4}{9} \times 4340 = 1930$, where, $N_0 \approx 6920$ is the number of muons in the ring at the start of the fill, and $t_{\text{fill}} \approx 30 \mu\text{sec}$ is the time it takes to fill the ring [2, 19]. The muon lifetime in the haloscope rest frame is $T = \gamma_\mu \tau_\mu = 64.4 \mu\text{sec}$, where, $\gamma_\mu \approx p_\mu/(m_\mu c) = 29.3$ is the muon time dilation factor, $p_\mu = 3.10 \text{ GeV}$ is the muon momentum, $m_\mu = 0.106 \text{ GeV}$ is the muon rest mass, and $\tau_\mu = 2.20 \mu\text{sec}$ is the muon life-time at rest [2]. For the measurements at Brookhaven E821 (BNL) [3], we estimate $N = 1290$, $\sigma_x = 2.10 \text{ cm}$, $\sigma_y = 1.53 \text{ cm}$ (J. Mott, private communication). To find the shift of muon spin precession from halo axions, we first computed $|\Delta a_\mu(\text{FNAL})| = (189 \pm 23) \times 10^{-11}$ and $|\Delta a_\mu(\text{BNL})| = (185 \pm 23) \times 10^{-11}$ for each experiment using Eq. (3). Next we took the average of the two experiments to obtain Δa_μ , since the shifts essentially agree. Finally, the uncertainty in the shift is set mainly by the axion-photon coupling and axion energy density. These uncertainties are correlated between the two experiments, so we take the uncertainty of Δa_μ to match that of the shifts seen by the individual experiments.
- [19] T. Albahri, A. Anastasi, K. Badgley, S. Baessler, I. Bailey *et al.* (Muon $g-2$ Collaboration), Beam dynamics corrections to the Run-1 measurement of the muon anomalous magnetic moment at Fermilab, *Phys. Rev. Accel. Beams* **24**, 044002 (2021).
- [20] T. Albahri, A. Anastasi, A. Anisenkov, K. Badgley, S. Baessler *et al.* (Muon $g-2$ Collaboration), Measurement of the anomalous precession frequency of the muon in the Fermilab Muon $g-2$ Experiment, *Phys. Rev. D* **103**, 072002 (2021).
- [21] We follow the analysis reviewed by R. D. Peccei [7] and set the ratio of axion couplings $g_{A\rho\omega}/g_{A\gamma\gamma} = g_{\pi\rho\omega}/g_{\pi\gamma\gamma}$ to match that of the neutral pion. Vector meson dominance [22] gives the pion ratio in terms of the ρ and ω vector meson partial widths for electron-positron pair production, as shown in Eq. (4). The electron-positron quantities entering Eq. (4) may be expressed in terms of the collider parameters: $N_e = \sqrt{N_+ N_-}$ where N_+ (N_-) is the number of positrons (electrons) per bunch, $V_e = 8\pi\sigma_x\sigma_y\sigma_z$ where $\sigma_x, \sigma_y, \sigma_z$ are the horizontal, vertical, and longitudinal sizes of the bunch at the interaction point, and $T_e = 2\sigma_z/c$.
- [22] R. P. Feynman, *Photon-Hadron Interactions* (Perseus, 1972), pp. 82–85 introduces the couplings $g_V = \alpha\sqrt{4\pi m_V}/(3\Gamma_V^{ee})$ for $V = \rho, \omega$ and pp. 96–97 expresses the pion amplitude ratio $g_{\pi\rho\omega}/g_{\pi\gamma\gamma} = g_\rho g_\omega/(4\pi e^2)$ in terms of these couplings and the electric charge e . Note that $e^2 = \alpha = 1/137$ in units with $\hbar = c = 1$.
- [23] V. Shiltsev and F. Zimmerman, 32. High Energy Collider Parameters in P. A. Zyla *et al.* (Particle Data Group), *Prog. Theor. Exp. Phys.* **2020**, 083C01 (2021).
- [24] The meson parameters [25] are $m_\rho = 775 \text{ MeV}$, $m_\omega = 783 \text{ MeV}$, $\Gamma_\rho^{ee} = \Gamma_\rho \times \text{B.R.}(\rho \rightarrow e^+e^-) = (147 \text{ MeV})(4.72 \times 10^{-5}) = 6.94 \text{ keV}$, and $\Gamma_\omega^{ee} = \Gamma_\omega \times \text{B.R.}(\omega \rightarrow e^+e^-) = (8.68 \text{ MeV})(7.38 \times 10^{-5}) = 0.641 \text{ keV}$. The electron-positron beam parameters are those inside the KLOE detector at the DAΦNE collider [23]: $N_+ = 2.1 \times 10^{10}$, $N_- = 3.2 \times 10^{10}$, $\sigma_x = 260 \mu\text{m}$, $\sigma_y = 4.8 \mu\text{m}$, and $\sigma_z = 2 \text{ cm}$. Hadron production detected by KLOE at the ρ meson $\pi^+\pi^-$ resonance lies close to the world average for this channel which dominates the a_μ^{HLO} calculation within the standard model [5]. Combining using the expressions in [20], one finds $N = \sqrt{N_+ N_-} = 2.6 \times 10^{10}$, $V = 6.3 \times 10^{-4} \text{ cm}^3$ and $T = 1.3 \times 10^{-4} \mu\text{sec}$.

- [25] R. L. Workman *et al.* (Particle Data Group), to be published in *Prog. Theor. Exp Phys.* **2022**, 083C01 (2022).
- [26] The radio-frequency magnetic field points along the infrared electric field.
- [27] M. Bialek, A. Magrez, A. Murk, and J.-Ph. Ansermet, Spin-wave resonances in bismuth orthoferrite at high temperatures, *Phys. Rev. B* **97**, 054410 (2018).
- [28] The electromagnon θ resonates when the terahertz magnetic field B_{THz} points along the spontaneous polarization P_{DC} : See Eq. (10), Fig. 2, and accompanying discussion on pg. 3 of R. de Sousa and J. E. Moore, Optical coupling to spin waves in the cycloidal multiferroic BiFeO_3 , *Phys. Rev. B* **77**, 012406 (2008). The axion down-converts the red-detuned infrared photon to terahertz frequency and aligns the magnetic field B_{THz} with the infrared electric field E_{IR} . Thus, the infrared absorption occurs for light polarized along the spontaneous polarization P_{DC} .